

Genuine Bistability in Open Quantum Many-Body Systems

Javad Kazemi* and Hendrik Weimer†

Institut für Theoretische Physik, Leibniz Universität Hannover, Appelstraße 2, 30167 Hannover, Germany

We analyze the long-time evolution of open quantum many-body systems using a variational approach. For the dissipative Ising model, where mean-field theory predicts a wide region of bistable behavior, we find genuine bistability only at a singular point, confirming the previously suggested picture of a first order transition. The situation is dramatically different when considering a majority-voter model including three-body interactions, where we find bistable behavior in an extended region, owing to the breaking of detailed balance in the effective description of the system. In this model, genuine bistability persists even when quantum fluctuations are added.

The metaphorically eternal lifetime of thermodynamically unstable diamond gemstones tells us that the minimum free energy is not the only thing that matters when considering the long-time properties of a physical system. Sufficiently large activation barriers can prevent the spontaneous decay of a metastable state even on astronomically large timescales. Here we show that similar behavior can also occur for the steady states of open quantum many-body systems, resolving a long-standing controversy about the existence and limits of bistable behavior in these systems.

In the context of open quantum many-body systems, bistable behavior in the steady state over an extended parameter range is predicted for many different systems by mean-field calculations [1–8]. However, these findings have so far not held up when using more elaborate methods [9–16]. This failure of mean-field theory can be partly understood using the variational principle for open systems [9], which allows for the formulation of steady state problems in terms of effective free energy functionals [17]. In this setting, one can see that mean-field solutions for open systems do not correspond to the physics above the upper critical dimension, as it is the case for equilibrium problems. However, the question whether other open quantum systems can support true bistability has remained unsolved.

In this Letter, we present a generic framework for describing the long-time evolution of open quantum many-body systems. For this, we establish a Gutzwiller approach for open quantum systems and employ the variational principle for a mapping onto an effective classical problem. In the presence of a dynamical symmetry [18], fluctuations exhibit thermal statistics, allowing us to employ the statistical theory of metastability [19]. For the dissipative Ising model exhibiting mean-field bistability [1, 3], we demonstrate that the thermodynamically unstable solution eventually decays except around a singular point, confirming the previously suggested picture of a first-order jump in the magnetization [9, 13, 14]. However, the situation is fundamentally different when considering a majority-voter model known as Toom’s model [20], which has recently found applications in topological quantum error correction [21–23] and the realization of

time crystals in open systems [24]. For this classical spin model, Monte-Carlo simulations have reported bistable behavior [25], which we also observe within our variational approach. We find this behavior being driven by the breaking of detailed balance in the non-equilibrium steady state, which we analyze based on an effective Langevin equation built upon the variational principle. Crucially, we also observe that bistability over an extended region persists under the inclusion of quantum fluctuations in terms of a Hamiltonian driving, constituting the first example of a true bistable phase in an open quantum many-body system.

Gutzwiller theory for open systems.— The Markovian evolution of quantum states in the form of a density matrix ρ can be described by the Liouvillian superoperator $\partial_t \rho = \mathcal{L}(\rho)$, in terms of the Lindblad master equation

$$\mathcal{L}(\rho) = -i[H, \rho] + \sum_j \left[c_j^\dagger \rho c_j - \frac{1}{2} \{c_j^\dagger c_j, \rho\} \right], \quad (1)$$

where H is the Hamiltonian of the system and the set of c_j s represents the jump operators [26]. This dynamics produces non-equilibrium steady states corresponding to $\mathcal{L}(\rho_s) = 0$. To approximate these states, we consider a Gutzwiller variational ansatz $\rho_v = \prod_i^N \rho_0$, where for spin-1/2 particles $\rho_0 \equiv \left(I + \sum_{\mu \in \{x, y, z\}} \alpha_\mu \sigma_\mu \right) / 2$ is expanded in terms of Pauli matrices σ_μ , while the corresponding coefficients α_μ are a set of variational parameters. These parameters can be obtained by minimizing a suitable variational cost function. Here, we consider a cost function derived from the vectorized form $\langle\langle \mathcal{L}^\dagger(\rho) | \mathcal{L}(\rho) \rangle\rangle$ in terms of the operator inner product $\text{Tr}\{A^\dagger B\} = \langle\langle A^\dagger | B \rangle\rangle$ inducing the Hilbert-Schmidt norm $\|A\|_2 = \sqrt{\text{Tr}\{A^\dagger A\}}$. However, as the Hilbert-Schmidt norm is biased towards the maximally mixed state [9], we normalize the cost function by the total purity $\text{Tr}[\rho^2] = \text{Tr}[\rho_0^2]^N$ to counteract the bias [27], i.e. $F_v = \langle\langle \mathcal{L}^\dagger(\rho) | \mathcal{L}(\rho) \rangle\rangle / \langle\langle \rho_0 | \rho_0 \rangle\rangle^N$.

For a given (uniform) Liouvillian we can express the square of the Hilbert-Schmidt norm $\|A\|_2^2$ as an expansion of its individual terms, geometrical different configurations as it is shown in fig. 1, which in turn can be factorized by some N - and N^2 -dependent coefficients.

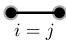
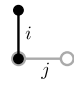
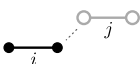
$\langle\langle \tilde{\mathcal{L}}_i^\dagger(\rho) \tilde{\mathcal{L}}_j(\rho) \rangle\rangle$			
$n_{ij} \equiv \dim(\rho)$	2	3	4
number of configurations	$\frac{z}{2}N$	$z(z-1)N$	$(\frac{z}{2}N)^2 - z(z-\frac{1}{2})N$

FIG. 1. Spatial configurations corresponding to a 2-local Liouvillian appearing on a 2D lattice with the coordination number $z = 4$. The black 2-dot lines labelled with i represent $\langle\langle \tilde{\mathcal{L}}_i^\dagger(\rho) |$ and the gray lines labelled with j represent $|\tilde{\mathcal{L}}_j(\rho)\rangle\rangle$ in the HS norm.

N -dependent configurations correspond to those terms in $\langle\langle \mathcal{L}^\dagger(\rho) | \mathcal{L}(\rho) \rangle\rangle$ where (fully/partially) mutual lattice sites are acted upon by some elements of \mathcal{L}^\dagger and \mathcal{L} while N^2 -dependent configurations represent non-overlapping terms. In addition, these coefficients also encode the lattice dimensionality via their dependency on the coordination number z . As a further step to have a scale-independent variational norm, which is required in this study, we treat these coefficients on the same footing, rescaling the N^2 -dependent term to N and then normalize the whole function by N . This step can be justified based on the fact that for short-range interacting system the N -dependent terms are dominant as they incorporate the overlapping inner products. As a result, the variational norm can be cast into the form

$$f_v = \sum_{ij} \frac{\langle\langle \tilde{\mathcal{L}}_i^\dagger(\rho) | \tilde{\mathcal{L}}_j(\rho) \rangle\rangle}{\langle\langle \rho_0 | \rho_0 \rangle\rangle^{n_{ij}}}, \quad (2)$$

where $\tilde{\mathcal{L}}_i$'s are individual terms in the Liouvillian, similar to what is depicted in fig. 1 and the denominator represents the local purity $\langle\langle \rho_0 | \rho_0 \rangle\rangle$ to the power of n_{ij} being the total dimension of the terms in the numerator.

In cases where the coherent and dissipative couplings are uniform, the variational norm can be evaluated analytically for generic Liouvillians even in the thermodynamic limit, analogous to Gutzwiller energies in ground state problems [28]. This property is in contrast with the more natural trace norm $\|A\|_1 = \text{Tr}\{|A|\}$, where additional approximations have to be applied to evaluate the variational norm [9, 10].

Thermally-activated nucleation processes. — In cases where the variational norm vanishes, the product state solution is an exact steady state of the system. Hence, the value of the variational norm gives direct access to the scale of fluctuations within the system [17]. For the first model studied here, these fluctuations obey thermal statistics [18], i.e., they can be captured in terms of an effective temperature $T \sim f_v$, considering the fact that the variational norm is also an intensive quantity. Importantly, rewriting the steady state problem of an open quantum many-body systems in terms of a classical statistical mechanics problem allows to employ the vast

toolbox for treating the latter. This also applies to the non-equilibrium relaxation dynamics of metastable states [19]. Here, we first compute all local minima of the variational norm. The stability of a local minimum which is not the global one (i.e., a metastable state) can then be quantified in terms of the relaxation rate by which the metastable state relaxes into the global minimum solution.

To calculate the relaxation rate, we consider the path between the metastable minimum and the stable minimum in the variational manifold, which is passing through a saddle-point having a variational norm of f_v^{sp} . Then, in analogy with the statistical theory of the decay of metastable states [19], we can express the relaxation rate (per volume) of the metastable solution as

$$I = f_v^{sp} \left(\frac{f_v^m}{2\pi\lambda} \right)^{1/2} e^{-\tilde{E}_a/f_v^m}, \quad (3)$$

where f_v^m is the value of variational norm of the metastable state and λ is the curvature of a saddle-point in the activation energy, see below. The equivalent of the activation energy \tilde{E}_a is given here by the variational cost of a critical nucleus of the stable solution (created by random fluctuations) within a system in the metastable state. In the following, we estimate \tilde{E}_a based on classical nucleation theory [29]. By considering square-shaped nucleus with the length ℓ , we obtain

$$E_a = -\ell^2(f_v^m - f_v^s) + 4\ell(f_v^{sp} - f_v^m), \quad (4)$$

which respectively consists of a volume energy of the nucleus, with f_v^s being the value of variational norm of the stable state, and a surface tension of its domain wall [29]. \tilde{E}_a is then defined as the maximized activation energy with the critical length $\ell^* = 2(f_v^{sp} - f_v^m)/(f_v^m - f_v^s)$. Concerning the surface tension, we consider a localized sharp kink, in the order of the lattice spacing, separating the stable nucleus from the rest. We have numerically verified that employing a smooth kink using an additional gradient term does not result in any significant change. Finally, $\lambda = 2(f_v^m - f_v^s) > 0$ is defined as the second derivative of E_a with respect to ℓ [19].

Dissipative Ising model. — As the first concrete model, we turn to the paradigmatic dissipative Ising model, as it is a widely studied model, where mean-field bistability gives way to a first-order transition. Its Hamiltonian part is given by

$$H = \frac{g}{2} \sum_i \sigma_x^{(i)} + \frac{J}{4} \sum_{\langle ij \rangle} \sigma_z^{(i)} \sigma_z^{(j)}, \quad (5)$$

where g and J indicate the strength of the transverse field and of the Ising interaction, respectively. Dissipation is incorporated by adding spin flips in the form of quantum jump operators $c_i = \sqrt{\gamma} \sigma_-^{(i)}$ with the rate γ .

Within our variational approach, we can obtain approximative steady-state solutions by minimizing the

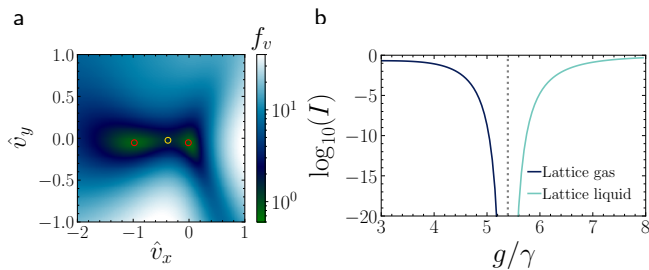


FIG. 2. (a) Variational norm f_v of the dissipative Ising model at the first-order transition ($J/\gamma = 5, g/\gamma = 5.40 \pm 0.01$) in a plane of transformed variational parameters $\hat{v}_x(\alpha_{x,y,z})$ and $\hat{v}_y(\alpha_{x,y,z})$ spanned by the two minima (red circles) and the intermediate saddle-point (yellow circle). The left and right minima correspond to the gas and liquid phase, respectively. (b) Logarithm of the relaxation rate $\log_{10}(I)$ of the metastable solution as a function of g/γ , showing a steep dip close to the phase transition.

variational norm f_v of Eq. (2). Close to the transition, our variational results show a double basin structure, see Fig. 2, indicating the presence of two competing phases (i.e., liquid and gas), separated by a saddle point. We note that our results for the position of the first-order transition are in excellent agreement with other calculations [9, 10, 13, 15, 16]. Crucially, the value of the variational norm at the two minima is different except exactly at the first-order transition. To analyze the fate of the metastable state (i.e., the local minimum with the higher variational norm), we compute the relaxation rate defined in eq. (3) to quantitatively assess long-time stability of the metastable solution. As shown in fig. 2b, the rate is finite far away from the transition and the metastable solution quickly relaxes into the stable one. However, for a narrow width of g/γ , the relaxation rate of the metastable state drastically decreases, explaining the experimentally observed hysteresis close to the transition [30]. However, this long-lasting metastability is not a genuine thermodynamic phase, as the relaxation rate is an analytic function over the entire parameter range.

Toom's majority voting model.— To answer the question whether it is possible to observe genuine bistability in an open quantum system, we turn to Toom's majority voting model, which supports bistability in a classic non-equilibrium setting [20, 25, 31, 32]. This model has recently found renewed interest because of its relevance for topological quantum error correction [21–23] and time crystals in open systems [24]. We explain how genuine bistability arises in Toom's model within our variational framework and show that this bistability is robust under the addition of quantum fluctuations. Toom's model is a set of classical rate equations for a system of binary variables (i.e., 0 and 1), which can be cast into a fully dissipative (i.e., $H = 0$) Lindblad master equation, gov-

erned by the jump operators

$$c_{j,\mu} = \sqrt{\gamma_\mu} \sigma_-^j M_0^{(j,j+E,j+N)} \quad (6)$$

$$c_{j,\bar{\mu}} = \sqrt{\bar{\gamma}_\mu} \sigma_+^j M_0^{(j,j+E,j+N)} \quad (7)$$

$$c_{j,\nu} = \sqrt{\gamma_\nu} \sigma_+^j M_1^{(j,j+E,j+N)} \quad (8)$$

$$c_{j,\bar{\nu}} = \sqrt{\bar{\gamma}_\nu} \sigma_-^j M_1^{(j,j+E,j+N)} \quad (9)$$

where $\sigma_- = |0\rangle\langle 1|$ and $\sigma_+ = |1\rangle\langle 0|$ are the lowering and raising operators, respectively, acting on the site j on a square lattice, depending on the state of j and its northern and eastern neighbors, expressed in terms of the majority vote operators M_s . Here, M_0 and M_1 refer to the configurations of the three sites where the majority is in the 0 and 1 state, respectively, see Tab. I for all possible configurations. Importantly, rates with index μ and ν refer to lowering and raising operations, respectively, while barred and unbarred rates are operations against and with the majority, respectively.

While the deterministic limit of Toom's model, i.e. $\bar{\gamma}_\mu = \bar{\gamma}_\nu = 0$ can readily eliminate minority islands, Toom has rigorously proved that this ability persists even in the presence of updates against the majority rule, provided that the probability of such events is sufficiently low [20, 33]. This makes Toom's model a fault-tolerant error correcting model for a finite range of the noise [22]. Although Toom's original proof is only relevant to the case where the sites are updated synchronously, it has been shown that the argument also holds for simultaneous updates in a master equation formalism [34].

Using a global evolution rate γ , Toom's model can be characterized in a dimensionless two-parameter space of noise and bias, according to the noise amplitude $T = e^{-\gamma_\nu/\gamma} + e^{-\gamma_\mu/\gamma}$, analogous to temperature, and with bias $h = (e^{-\gamma_\nu/\gamma} - e^{-\gamma_\mu/\gamma})/T$, analogous to a symmetry-breaking external magnetic field in the Ising model. In the case of unbiased noise $h = 0$, the model behaves like the zero-field Ising model with a continuous transition at a critical temperature. However, even at the presence of biased noise the model undergoes a first-order transition between a bistable phase and a unique ergodic phase. This behavior arises from the chirality of the jump operators in Eq. (9), as they do not contain the west and south sites [35, 36]. Basically, any chiral updating rule leads to a violation of the detailed balance condition, which is necessary when trying to obtain a stationary state that does not exhibit thermal statistics [32].

NCE state	101	111	110	011	010	100	001	000
Operation	σ_+	σ_-	σ_-	σ_-	σ_-	σ_+	σ_+	σ_+
rate	γ_ν	$\bar{\gamma}_\nu$	$\bar{\gamma}_\nu$	$\bar{\gamma}_\nu$	γ_μ	$\bar{\gamma}_\mu$	$\bar{\gamma}_\mu$	$\bar{\gamma}_\mu$

TABLE I. Ruleset and the corresponding transition rates for Toom's model indicating how the central site is updated according to the North-Center-East (NCE) state.

In the presence of thermal statistics, it is relatively straightforward to express the variational norm of Eq. (2) in terms of a Ginzburg-Landau-Wilson framework and then apply standard techniques for the study of critical phenomena such as a perturbative renormalization group treatment [17] to obtain the steady-state phase diagram. However, we cannot take this route here as the lack of detailed balance can lead to non-thermal steady states. To overcome this obstacle, we introduce a Langevin equation to describe the full relaxation dynamics of the observables $\phi_i = \langle \sigma_z^{(i)} \rangle$. To this end, we first perform a gradient expansion of the variational norm, i.e., $f_v(\{\phi_i\}) = \sum_i f_i(\phi_i, \nabla \phi_i)$, where $\nabla \phi_i = (\phi_{i+E} - \phi_i, \phi_{i+N} - \phi_i)$ is the lattice gradient [37]. The Langevin equation is then given by $\partial_t \phi_i = -\partial f_v / \partial \phi_i + \xi_i$, yielding

$$\frac{\partial}{\partial t} \phi_i = - \left[\frac{\partial f_0}{\partial \phi_i} - a - (b-b') \nabla \phi_i - 2b' \phi_i - c \nabla^2 \phi_i \right] + \xi_i, \quad (10)$$

where f_0 denotes the variational norm for the homogeneous case without any gradient terms and ξ_i is a white Gaussian noise, i.e. $\langle \xi_i \rangle = 0$ and $\langle \xi_i(t) \xi_j(0) \rangle = f_0^m \delta_{i,j} \delta(t)$ with f_0^m (the variational norm of the metastable solution) as the effective temperature [37]. Furthermore, we have truncated the gradient expansion at second order. Our Langevin equation differs from that of conventional kinetic Ising models [38] due to the appearance of a linear gradient term with coefficient $(b-b') > 0$ which captures the chirality of the jump operators. Here, a sufficiently large $(b-b')$ ensures the shrinkage of minority islands of either states. Importantly, similar Langevin equations for the Toom's model have already been proposed on a purely phenomenological level [35], while in our variational approach, all coupling constants can be directly calculated from the microscopic model. We also note that our Langevin equation is on equal footing to those that can be derived within the Keldysh formalism [39], however, performing such calculations for spin systems is often challenging because of the hard-core constraint imposed by spins [40].

We are now in the position to calculate the phase diagram of Toom's model in the $T-h$ plane by solving the Langevin equation for a 20×20 lattice and averaging over 100 samples initialized in a configuration polarized against the bias field [37]. Fig. 3 demonstrates an extended region of bistability in the absence of the Z_2 symmetry of the Ising model that has no counterpart in the corresponding equilibrium system. We note that due to the asynchronicity of master equation in contrast to the Toom's original updating rules, the phase diagram quantitatively differs from that of the synchronous model [25], but the qualitative behavior is identical. According to the numerical simulation close to criticality, two lines separate the bistable region from the ergodic one ending up to an Ising critical point at $T_c = 0.777 \pm 0.001$ on the $h = 0$ line, as shown in the inset of Fig. 3.

Having shown that our variational approach is able to

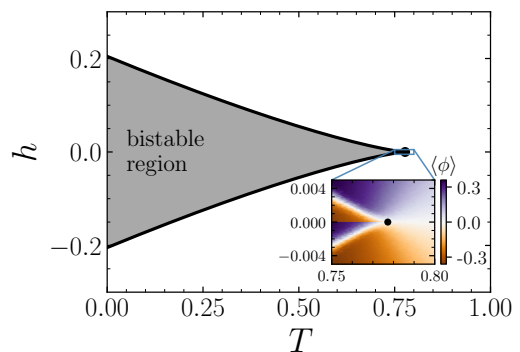


FIG. 3. Phase diagram of The Toom's model shows two phase transition lines separating a bistable phase (gray) from an ergodic phase (white), meeting at a critical point at $T_c = 0.777 \pm 0.001$ (black dot). The inset shows how the orientation of stationary magnetization (starting from a majority of sites polarized against the bias) changes in different zones close to criticality.

reproduce the phase diagram of the classical model, we now turn to the addition of quantum fluctuations. In the context of Toom's model, this can be done in a natural way in terms of a PXP Hamiltonian of the form

$$H = \Omega \sum_j [P_0^{(j+N)} \sigma_x^{(j)} P_0^{(j+E)} + P_1^{(j+N)} \sigma_x^{(j)} P_1^{(j+E)}], \quad (11)$$

where $P_i = |i\rangle\langle i|$ is a projection operator acting on the northern and eastern neighbors. Such PXP terms are of great interest in the investigation of strongly interacting Rydberg systems [41–43], while the realization of the jump operators of Eq. (9) is also feasible within these systems [44]. In the language of Toom's model, these quantum fluctuations act against the local majority and therefore provide a new source of quantum noise to the update rules. Additionally, the Hamiltonian conserves σ_x on all sites, hence the variational Gutzwiller ansatz can be parameterized using only α_y and α_z . We first perform a rotation of the variational parameters according to $\phi = \cos(\theta)\alpha_z + \sin(\theta)\alpha_y$ with $\theta = \arctan(\alpha_y/\alpha_z)$. Importantly, this rotation results in ϕ containing all the critical behavior of the system, while the orthogonal field ϕ_\perp can be approximated by a quadratic term close to the variational minima, see Fig. 4, i.e., it is always gapped. Importantly, while quantum fluctuations lead to a renormalization of the coupling constants of the Langevin equation for ϕ , its form remains unchanged.

To obtain the phase diagram in the presence of quantum fluctuations, we first compute the homogeneous variational norm f_v in terms of α_y and α_z . Figs. 4a and 4b show the variational landscape deep in the bistable phase and the ergodic phase, respectively. We then compute the phase diagram in the $\Omega-h$ plane close to the Ising critical point at $T = 0.75$, see Fig. 4c. Crucially,

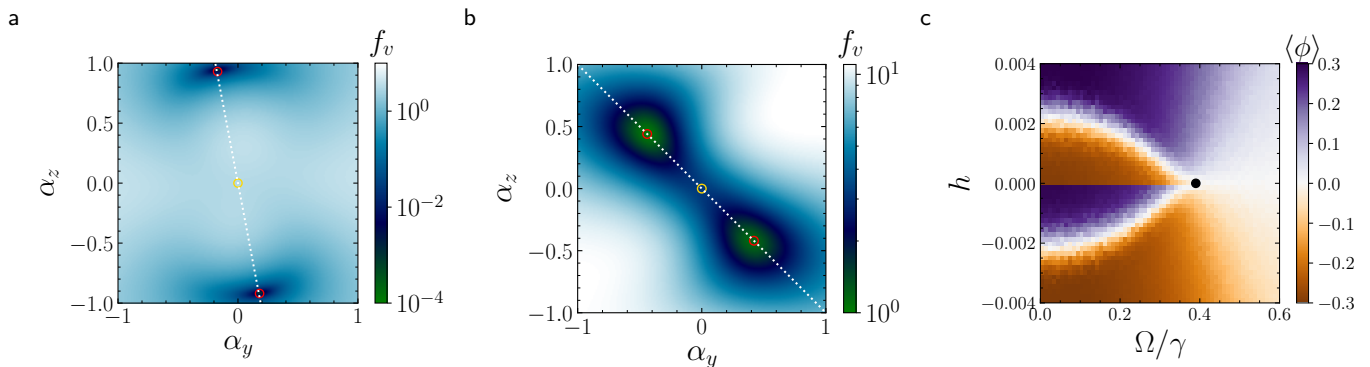


FIG. 4. Bistability in the variational steady state of Toom's model in the presence of quantum fluctuation. Variational norm (in logarithmic scale) is depicted as a function of α_z and α_y for $H = T = 0.15$ deep in (a) the bistable phase with $\Omega/\gamma = 0.15$ and (b) the ergodic phase with $\Omega/\gamma = 2.0$. The dotted lines show the axis of the effective classical field. (c) Phase diagram in the presence of quantum fluctuations at $T = 0.75$ showing gradual shrinkage of the bistable region by increasing Ω ending up with a critical point (black square) at $\Omega_c/\gamma = 0.39 \pm 0.02$ similar to the classical case.

we find extended bistability even in the presence of quantum fluctuations. Essentially, deep in the bistable region (Fig. 4a), small amounts of quantum fluctuations cannot overcome the bistability barrier because the strength of the fluctuations indicated by the variational norm f_v is very small. However, by increasing Ω (Fig. 4b), both the strength of the fluctuation increases substantially and the barrier separating the two variational minima is greatly decreased, leading to ergodic behavior. Finally, similar to the classical case, the phase boundaries separating the bistable from the ergodic phase meet in a critical point on the Z_2 -symmetric line given by $h = 0$. We have also investigated the phase diagram for different Hamiltonian perturbations such as a transverse field proportional to σ_x , where we find qualitatively similar behavior. This suggests that Toom's model can serve as an error-correcting code in the presence of generic quantum fluctuations.

To summarize, we have developed a method for assessing the long-time evolution of open many-body systems. In the presence of a dynamical symmetry giving rise to thermal statistics of the steady state, one can calculate the relaxation rate using a statistical approach built on classical nucleation theory. In the absence of the dynamical symmetry, we find that the time evolution of the system can be captured in terms of an effective Langevin equation, which allows to map out the steady-state phase diagram of systems violating detailed balance, where we find the first instance of genuine bistability in an open quantum system when adding quantum fluctuations to Toom's majority voting model. Our approach can be used for many other critical systems that are otherwise inherently difficult to treat, such as quantum contact processes [45], systems exhibiting limit cycles [46], or neural networks based on open quantum systems [47].

This work was funded by the Volkswagen Foundation,

by the Deutsche Forschungsgemeinschaft (DFG, German Research Foundation) within Project-ID 274200144 – SFB 1227 (DQ-mat, Project No. A04), SPP 1929 (GiRyd), and under Germany's Excellence Strategy–EXC-2123 QuantumFrontiers–390837967.

* javad.kazemi@itp.uni-hannover.de

† hweimer@itp.uni-hannover.de

- [1] T. E. Lee, H. Häffner, and M. C. Cross, Antiferromagnetic phase transition in a nonequilibrium lattice of Rydberg atoms, *Phys. Rev. A* **84**, 031402(R) (2011).
- [2] T. E. Lee and M. C. Cross, Spatiotemporal dynamics of quantum jumps with Rydberg atoms, *Phys. Rev. A* **85**, 063822 (2012).
- [3] M. Marcuzzi, E. Levi, S. Diehl, J. P. Garrahan, and I. Lesanovsky, Universal Nonequilibrium Properties of Dissipative Rydberg Gases, *Phys. Rev. Lett.* **113**, 210401 (2014).
- [4] A. Le Boité, G. Orso, and C. Ciuti, Steady-State Phases and Tunneling-Induced Instabilities in the Driven Dissipative Bose-Hubbard Model, *Phys. Rev. Lett.* **110**, 233601 (2013).
- [5] J. Jin, D. Rossini, R. Fazio, M. Leib, and M. J. Hartmann, Photon Solid Phases in Driven Arrays of Nonlinearly Coupled Cavities, *Phys. Rev. Lett.* **110**, 163605 (2013).
- [6] A. Le Boité, G. Orso, and C. Ciuti, Bose-Hubbard model: Relation between driven-dissipative steady states and equilibrium quantum phases, *Phys. Rev. A* **90**, 063821 (2014).
- [7] T. Mertz, I. Vasić, M. J. Hartmann, and W. Hofstetter, Photonic currents in driven and dissipative resonator lattices, *Phys. Rev. A* **94**, 013809 (2016).
- [8] C. D. Parmee and N. R. Cooper, Phases of driven two-level systems with nonlocal dissipation, *Phys. Rev. A* **97**, 053616 (2018).
- [9] H. Weimer, Variational Principle for Steady States of Dis-

- sipative Quantum Many-Body Systems, *Phys. Rev. Lett.* **114**, 040402 (2015).
- [10] H. Weimer, Variational analysis of driven-dissipative Rydberg gases, *Phys. Rev. A* **91**, 063401 (2015).
- [11] J. J. Mendoza-Arenas, S. R. Clark, S. Felicetti, G. Romero, E. Solano, D. G. Angelakis, and D. Jaksch, Beyond mean-field bistability in driven-dissipative lattices: Bunching-antibunching transition and quantum simulation, *Phys. Rev. A* **93**, 023821 (2016).
- [12] M. F. Maghrebi and A. V. Gorshkov, Nonequilibrium many-body steady states via Keldysh formalism, *Phys. Rev. B* **93**, 014307 (2016).
- [13] A. Kshetrimayum, H. Weimer, and R. Orús, A simple tensor network algorithm for two-dimensional steady states, *Nature Commun.* **8**, 1291 (2017).
- [14] M. Raghunandan, J. Wrachtrup, and H. Weimer, High-Density Quantum Sensing with Dissipative First Order Transitions, *Phys. Rev. Lett.* **120**, 150501 (2018).
- [15] J. Jin, A. Biella, O. Viyuela, C. Ciuti, R. Fazio, and D. Rossini, Phase diagram of the dissipative quantum Ising model on a square lattice, *Phys. Rev. B* **98**, 241108(R) (2018).
- [16] V. P. Singh and H. Weimer, Driven-dissipative criticality within the discrete truncated Wigner approximation, [arXiv:2108.07273](https://arxiv.org/abs/2108.07273) (2021).
- [17] V. R. Overbeck, M. F. Maghrebi, A. V. Gorshkov, and H. Weimer, Multicritical behavior in dissipative Ising models, *Phys. Rev. A* **95**, 042133 (2017).
- [18] L. M. Sieberer, S. D. Huber, E. Altman, and S. Diehl, Dynamical Critical Phenomena in Driven-Dissipative Systems, *Phys. Rev. Lett.* **110**, 195301 (2013).
- [19] J. Langer, Statistical theory of the decay of metastable states, *Ann. Phys.* **54**, 258 (1969).
- [20] A. L. Toom, in *Multicomponent Random Systems*, edited by R. L. Dobrushin and Y. G. Sinai (Marcel Dekker, New York, 1980) pp. 549–575.
- [21] M. Herold, M. J. Kastoryano, E. T. Campbell, and J. Eisert, Cellular automaton decoders of topological quantum memories in the fault tolerant setting, **19**, 063012 (2017).
- [22] A. Kubica and J. Preskill, Cellular-Automaton Decoders with Provable Thresholds for Topological Codes, *Phys. Rev. Lett.* **123**, 020501 (2019).
- [23] M. Vasmer, D. E. Browne, and A. Kubica, Cellular automaton decoders for topological quantum codes with noisy measurements and beyond, *Scientific Reports* **11** (2021).
- [24] Q. Zhuang, F. Machado, N. Y. Yao, and M. P. Zaletel, An absolutely stable open time crystal (2021), [arXiv:2110.00585](https://arxiv.org/abs/2110.00585) [quant-ph].
- [25] C. H. Bennett and G. Grinstein, Role of Irreversibility in Stabilizing Complex and Nonergodic Behavior in Locally Interacting Discrete Systems, *Phys. Rev. Lett.* **55**, 657 (1985).
- [26] H.-P. Breuer and F. Petruccione, *The Theory of Open Quantum Systems* (Oxford University Press, Oxford, 2002).
- [27] F. Vicentini, A. Biella, N. Regnault, and C. Ciuti, Variational neural network ansatz for steady states in open quantum systems, [arXiv e-prints](https://arxiv.org/abs/1902.10104), [arXiv:1902.10104](https://arxiv.org/abs/1902.10104) (2019).
- [28] W. Krauth, M. Caffarel, and J.-P. Bouchaud, Gutzwiller wave function for a model of strongly interacting bosons, *Physical Review B* **45**, 3137 (1992).
- [29] P. M. Chaikin and T. C. Lubensky, *Principles of condensed matter physics* (Cambridge University Press, Cambridge, 1995).
- [30] C. Carr, R. Ritter, C. G. Wade, C. S. Adams, and K. J. Weatherill, Nonequilibrium Phase Transition in a Dilute Rydberg Ensemble, *Phys. Rev. Lett.* **111**, 113901 (2013).
- [31] P. Gács and J. Reif, A simple three-dimensional real-time reliable cellular array, *Journal of Computer and System Sciences* **36**, 125 (1988).
- [32] G. Grinstein, Can complex structures be generically stable in a noisy world?, *IBM J. Res. Dev.* **48**, 5 (2004).
- [33] J. L. Lebowitz, C. Maes, and E. R. Speer, Statistical mechanics of probabilistic cellular automata, *J. Stat. Phys.* **59**, 117 (1990).
- [34] L. F. Gray, Toom’s Stability Theorem in Continuous Time, in *Perplexing Problems in Probability: Festschrift in Honor of Harry Kesten*, edited by M. Bramson and R. Durrett (Birkhäuser Boston, Boston, MA, 1999) pp. 331–353.
- [35] Y. He, C. Jayaprakash, and G. Grinstein, Generic nonergodic behavior in locally interacting continuous systems, *Phys. Rev. A* **42**, 3348 (1990).
- [36] M. A. Muñoz, F. de los Santos, and M. M. Telo da Gama, Generic two-phase coexistence in nonequilibrium systems, *Eur. Phys. J. B* **43**, 73 (2005).
- [37] See the Supplemental Material for the gradient expansion of Toom’s model, the detailed derivation of the Langevin equation, and the choice of the initial state.
- [38] P. C. Hohenberg and B. I. Halperin, Theory of dynamic critical phenomena, *Rev. Mod. Phys.* **49**, 435 (1977).
- [39] L. M. Sieberer, M. Buchhold, and S. Diehl, Keldysh field theory for driven open quantum systems, *Rep. Prog. Phys.* **79**, 096001 (2016).
- [40] M. N. Kiselev and R. Oppermann, Schwinger-Keldysh Semicion Approach for Quantum Spin Systems, *Phys. Rev. Lett.* **85**, 5631 (2000).
- [41] B. Sun and F. Robicheaux, Numerical study of two-body correlation in a 1D lattice with perfect blockade, *New J. Phys.* **10**, 045032 (2008).
- [42] C. J. Turner, A. A. Michailidis, D. A. Abanin, M. Serbyn, and Z. Papić, Weak ergodicity breaking from quantum many-body scars, *Nature Phys.* **14**, 745 (2018).
- [43] D. Bluvstein, A. Omran, H. Levine, A. Keesling, G. Semeghini, S. Ebadi, T. T. Wang, A. A. Michailidis, N. Maskara, W. W. Ho, S. Choi, M. Serbyn, M. Greiner, V. Vuletić, and M. D. Lukin, Controlling quantum many-body dynamics in driven Rydberg atom arrays, *Science* **371**, 1355 (2021).
- [44] T. M. Wintermantel, Y. Wang, G. Lochead, S. Shevate, G. K. Brennen, and S. Whitlock, Unitary and Nonunitary Quantum Cellular Automata with Rydberg Arrays, *Phys. Rev. Lett.* **124**, 070503 (2020).
- [45] F. Carollo, E. Gillman, H. Weimer, and I. Lesanovsky, Critical Behavior of the Quantum Contact Process in One Dimension, *Phys. Rev. Lett.* **123**, 100604 (2019).
- [46] E. T. Owen, J. Jin, D. Rossini, R. Fazio, and M. J. Hartmann, Quantum correlations and limit cycles in the driven-dissipative Heisenberg lattice, *New Journal of Physics* **20**, 045004 (2018).
- [47] P. Rotondo, M. Marcuzzi, J. P. Garrahan, I. Lesanovsky, and M. Müller, Open quantum generalisation of Hopfield neural networks, *J. Phys. A* **51**, 115301 (2018).

Supplemental Material for “Genuine Bistability in Open Quantum Many-Body Systems”

Javad Kazemi* and Hendrik Weimer†
Institut für Theoretische Physik, Leibniz Universität Hannover, Appelstraße 2, 30167 Hannover, Germany

VARIATIONAL GRADIENT EXPANSION FOR TOOM’S MODEL

We start by formulating a Ginzburg-Landau functional from the variational norm within the Gutzwiller theory for open quantum systems. We consider the functional as a discrete sum over lattice sites including the homogeneous variational norm f_0 as well as an inhomogeneous term f_∇ to incorporate spatial inhomogeneities, i.e.,

$$f_v(\{\phi_i\}) = \sum_i f_i(\phi_i, \nabla\phi_i) = f_0 + \sum_i f_\nabla(\phi_i, \nabla\phi_i), \quad (\text{S1})$$

where f_∇ is constructed by the overlapping terms of the Liouvillian, see Fig. S1, such that $f_\nabla(\nabla\phi_i = 0) = 0$, yielding

$$f_\nabla(\phi_i, \nabla\phi_i) = \sum_j \frac{\langle\langle \tilde{\mathcal{L}}_i^\dagger(\phi_i, \nabla\phi_i) | \tilde{\mathcal{L}}_j(\phi_i, \nabla\phi_i) \rangle\rangle - \langle\langle \tilde{\mathcal{L}}_i^\dagger(\phi_i) | \tilde{\mathcal{L}}_j(\phi_i) \rangle\rangle}{\langle\langle \rho_0(\phi_i) | \rho_0(\phi_i) \rangle\rangle^{n_{ij}}}, \quad (\text{S2})$$

with j running over both i and the nearest neighbors that are coupled via the action of the Liouvillian. We can express f_∇ in terms of the localized field ϕ_i and the spatial inhomogeneities around it, i.e. $\nabla\phi_i = \delta_x \hat{x} + \delta_y \hat{y}$, with

$$\begin{aligned} \delta_x &= (\phi_{i+E} - \phi_i) = -(\phi_{i+W} - \phi_i) \\ \delta_y &= (\phi_{i+N} - \phi_i) = -(\phi_{i+S} - \phi_i), \end{aligned} \quad (\text{S3})$$

where the capital letters denote the cardinal direction. For Toom’s model, performing a Taylor expansion of f_∇ around $\phi_i = 0$ up to the second order yields

$$f_\nabla = \frac{a}{2} [\delta_x + \delta_y] + b\delta_x\delta_y + b'\phi_i [\delta_x + \delta_y] + c[\delta_x^2 + \delta_y^2], \quad (\text{S4})$$

where a , b , b' , and c are the expansion coefficients of the variational norm. Using lattice gradients, this can be expressed as

$$f_\nabla = \left(\frac{a}{2} + b'\phi_i \right) \nabla\phi_i + b(\nabla\phi_i \cdot \hat{x})(\nabla\phi_i \cdot \hat{y}) + c(\nabla\phi_i)^2. \quad (\text{S5})$$

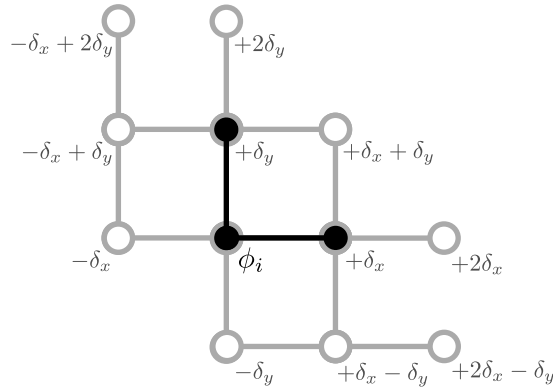


FIG. S1. Spatial gradients corresponding to the Toom’s model. Here, the black L shape represents $\langle\langle \tilde{\mathcal{L}}_i^\dagger |$ and the gray L shapes represent $|\tilde{\mathcal{L}}_j\rangle$ as a function of ϕ_i and its spatial gradients δ_x and δ_y .

* javad.kazemi@itp.uni-hannover.de

† hweimer@itp.uni-hannover.de

DERIVATION OF THE VARIATIONAL LANGEVIN EQUATION

To obtain the time evolution of a classical field $\phi(t) \equiv \phi_t$, we consider a generic density matrix $\rho(t)$ as a function of a small perturbation ϵ

$$\rho(t) = \frac{1}{2}[\rho(\phi_t + \epsilon) + \rho(\phi_t - \epsilon)]. \quad (\text{S6})$$

In the following, we consider the decay of the variational trial state ρ under the Lindbladian \mathcal{L} , i.e.,

$$\rho(t + \tau) = \exp(\mathcal{L}\tau)\rho(t) \approx \mathcal{N} \exp(-f_v\tau)\rho(t), \quad (\text{S7})$$

where \mathcal{N} is a normalization factor. Inserting Eq. (S6) yields

$$\rho(t + \tau) = \frac{e^{-f_v(\phi_t + \epsilon)\tau}\rho(\phi_t + \epsilon) + e^{-f_v(\phi_t - \epsilon)\tau}\rho(\phi_t - \epsilon)}{e^{-f_v(\phi_t + \epsilon)\tau} + e^{-f_v(\phi_t - \epsilon)\tau}}, \quad (\text{S8})$$

or equivalently, for the field ϕ

$$\phi_{t+\tau} = \frac{e^{-f_v(\phi_t + \epsilon)\tau}(\phi_t + \epsilon) + e^{-f_v(\phi_t - \epsilon)\tau}(\phi_t - \epsilon)}{e^{-f_v(\phi_t + \epsilon)\tau} + e^{-f_v(\phi_t - \epsilon)\tau}} \quad (\text{S9})$$

Performing a Taylor expansion around ϕ up to the second order, we arrive in the limit $\tau \rightarrow 0$ at

$$\frac{\partial}{\partial t}\phi = -\epsilon^2 \frac{\partial f_v}{\partial \phi}. \quad (\text{S10})$$

Here, ϵ can be interpreted to define a mesoscopic timescale. We can express the evolution of ϕ in the units of the mesoscopic timescale by performing the rescaling $\epsilon^2 t \rightarrow t$. Additionally, it is straightforward to generalize this expression to many-body systems containing multiple fields ϕ_i .

Importantly, the rescaled equation of motion for ϕ_i is not yet self-consistent as it lacks fluctuations. For self-consistency of the solution, the strength of fluctuations needs to correspond to the variational norm of the homogeneous solution [1]. This can be achieved by adding a stochastic term ξ to the equation of motion, i.e.,

$$\frac{\partial}{\partial t}\phi_i = -\left.\frac{\partial f_v}{\partial \phi}\right|_{\phi=\phi_i} + \xi_i, \quad (\text{S11})$$

where ξ_i is white Gaussian noise having zero mean and a correlation function given by $\langle \xi_i(t)\xi_j(t') \rangle = f_h(\phi_i)\delta_{i,j}\delta(t-t')$, with $f_h(\phi_i)$ denoting the variational norm of the homogeneous solution according to ϕ_i . Close to criticality, $f_h(\phi_i)$ can be replaced by the variational minimum f_0 . Then, the Langevin equation for Toom's model is given by

$$\frac{\partial}{\partial t}\phi_i = -\left[\frac{\partial f_0}{\partial \phi_i} - a - (b - b')\nabla\phi_i - 2b'\phi_i - c\nabla^2\phi_i\right] + \xi_i, \quad (\text{S12})$$

where the gradient terms indicate discrete lattice differences according to

$$\begin{aligned} \nabla\phi_i &= \phi_{i+N} + \phi_{i+E} - 2\phi_i, \\ \nabla^2\phi_i &= \phi_{i+N} + \phi_{i+S} + \phi_{i+W} + \phi_{i+E} - 4\phi_i. \end{aligned} \quad (\text{S13})$$

INITIAL STATE FOR VARIATIONAL SIMULATIONS

The bistability within Toom's model can be traced back to its ability to eliminate minority islands of arbitrary size. This elimination process is also independent of the island's shape. In Fig. S2, we illustrate this by solving the equation of motion for a lattice of 20×20 sites. As the initial state in the simulation, we consider a square-shape minority island with a length of 10 whose state is favored by the bias field h and the bulk being in the unfavored state. We observe that in the case of zero white noise, the square-shape island gradually turns into a triangle and then the aforementioned shrinkage takes place. While the white noise is very small only deep in the bistable region, the principal argument also holds close to criticality where the noise terms become important. Since all initial shapes are reduced to triangles on timescales much faster than the overall relaxation, we consider initial states that have a triangular minority island polarized along the bias field, while the majority of the initial state is polarized against

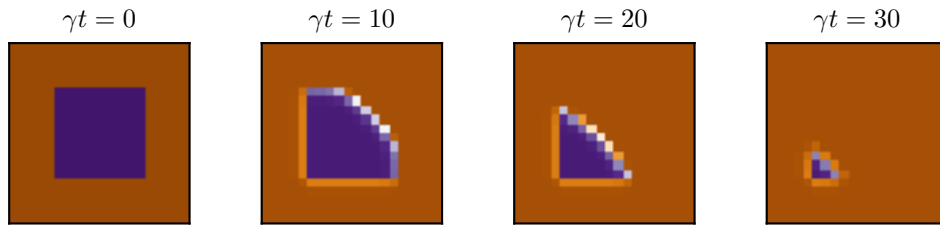


FIG. S2. Time evolution of a 10×10 minority island of the stable state encircled by the less-stable state on 20×20 square lattice with $T = 0.75$, $h = 0.001$ and zero white noise.

the bias. Specifically, we choose a triangle with a side length of 10 sites in a 20×20 lattice with periodic boundary conditions. We then solve the stochastic Langevin equation and average over 100 realizations.

-
- [1] V. R. Overbeck, M. F. Maghrebi, A. V. Gorshkov, and H. Weimer, Multicritical behavior in dissipative Ising models, *Phys. Rev. A* **95**, 042133 (2017).